

## 22. AN ASTRONOMICALLY CALIBRATED AGE MODEL FOR PLIOCENE SITE 1085, ODP LEG 175<sup>1</sup>

Beth A. Christensen<sup>2</sup> and Mark Maslin<sup>3</sup>

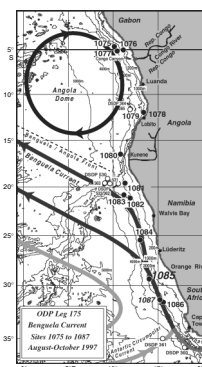
### ABSTRACT

An astronomically calibrated age model for the Pliocene section of Ocean Drilling Program Leg 175 Cape Basin Site 1085 based on magnetic susceptibility data was developed using shipboard biostratigraphic datums. The composite core magnetic susceptibility record was compiled using shipboard correlations between Holes 1085A and 1085B and then tuned to the record of orbital variations in eccentricity to generate an orbitally tuned age model. Magnetic susceptibility apparently records climate variations in the Cape Basin. Strong power spectra values at the 100- and 400-k.y. frequency suggest an orbital control on the beat of Pliocene climate change in the Cape Basin.

### INTRODUCTION

Shipboard studies suggest Pliocene sedimentation in the Cape Basin is approximately continuous at Site 1085 (Wefer, Berger, Richter, et al., 1998), so an orbitally tuned age model was developed to constrain the timing of the geochemical and lithologic changes in the Cape Basin using core and well log data. Geochemical and lithologic variations (Ellershaw et al., in press, this volume; Christensen et al., 1999; Kalbas et al., 1999; Wefer, Berger, and Richter, et al., 1998) suggest that the onset of Northern Hemisphere glaciation had a significant impact on the oceanography of the Cape Basin (Fig. F1). A high-resolution age model is necessary to identify the response of the Cape Basin to Northern Hemi-

F1. ODP Sites 1075–1087 drilled during Leg 175, p. 7.



<sup>1</sup>Christensen, B.A., and Maslin, M., 2001. An astronomically calibrated age model for Pliocene Site 1085, ODP Leg 175. *In* Wefer, G., Berger, W.H., and Richter, C. (Eds.), *Proc. ODP, Sci. Results*, 175, 1–19 [Online]. Available from World Wide Web: <[http://www-odp.tamu.edu/publications/175\\_SR/VOLUME/CHAPTERS/SR175\\_22.PDF](http://www-odp.tamu.edu/publications/175_SR/VOLUME/CHAPTERS/SR175_22.PDF)>. [Cited YYYY-MM-DD]

<sup>2</sup>Department of Earth and Environmental Sciences, Furman University, 3300 Poinsett Highway, Greenville SC 29613, USA.

[bchristensen@gsu.edu](mailto:bchristensen@gsu.edu)

Present address: Department of Geology, 24 Peachtree Center Avenue, Georgia State University, Atlanta GA 30303, USA.

<sup>3</sup>Environmental Change Research Centre and Benfield Greig Hazard Research Centre, Department of Geography, University College London, 26 Bedford Way, London, United Kingdom.

Initial receipt: 21 February 2000

Acceptance: 18 June 2001

Web publication: 20 November 2001

Ms 175SR-204

sphere glaciation and to compare the record of onset in both hemispheres.

This paper outlines the creation of an age model sufficient for high-resolution climate change studies on core material. It was generated by orbitally tuning the composite section and tested using standard techniques of spectral analysis. The spectral and cross-spectral analyses suggest a systemic relationship between deposition in the Cape Basin and orbital forcing; however, proxies are necessary to determine whether the relationship is coincident or causative. Thus, the final stage of the project, a comparison of the Cape Basin records with other records of climate change, particularly those in the Northern Hemisphere, will be the subject of a future paper.

## **MATERIALS AND METHODS**

Site 1085 was drilled in a water depth of 1713.2 m at 29°22'S, 13°59'E (Wefer, Berger, Richter, et al., 1998) (Fig. F1). Drilling at Hole 1085A penetrated a total of 604 meters below seafloor (mbsf) and recovered a relatively continuous section of calcareous nannofossil ooze, extending to the middle Miocene (Wefer, Berger, Richter, et al., 1998). Hole 1085B (29°22'S, 13°59'E) was drilled to 321.2 mbsf (Wefer, Berger, Richter, et al., 1998) and was used to create a composite record.

Shipboard calcareous nannofossil and planktonic foraminifer datums (see Table T1) were used to constrain the initial age model using core magnetic susceptibility (MS) records for the Pliocene section of Site 1085. Since the biostratigraphic (BIO) age model was based on shipboard datums determined from core-catcher material, the initial shipboard stratigraphic position is approximate and datum positions reflect at least a 9.5-m possible range of stratigraphic position. The MS was tuned to the eccentricity curve for the interval (Laskar, 1990) by matching the high-resolution MS record with increased insolation using Analyseries software (Paillard et al., 1996) to create the tuned core magnetic susceptibility (TCMS) age model (see Table T2 for the control points used to create the TCMS model). Both the BIO and the TCMS models were evaluated for Milankovitch periodicities using Analyseries software (Paillard et al., 1996) using both spectral and the cross-spectral methods. The Blackman-Tukey method of spectral analysis was used to identify the dominant periodicity in the BIO and TCMS age models. The analysis of the linear detrended age models was performed using a 2-k.y. step, bandwidth of 0.00139, and 2149 lags. Similar results were returned at both 80% and 95% confidence levels. Cross-spectral analysis between the eccentricity and TCMS records was also performed using Analyseries software (Paillard et al., 1996). The TCMS vs. eccentricity analysis was performed at 95% confidence level using a step of 0.5 k.y., 2100 lags, and a bandwidth of 0.00142 on linear detrended data.

The age models were developed using a composite MS record (Fig. F2) of Holes 1085A and 1085B to ensure analysis of a complete section. The composite was created by splicing multisensor track (MST) MS core records from Hole 1085A and Hole 1085B and was based on the splice that was developed shipboard (see Wefer, Berger, Richter, et al., 1998, for details on the construction of the shipboard composite record). A nine-point smoothing function was applied to the records. The composite section compensates for gaps due to drilling by overlapping records from adjacent holes and splicing them together to create what is ideally a complete record of deposition. The standard composite sec-

---

**T1.** Shipboard biostratigraphic datums, p. 16.

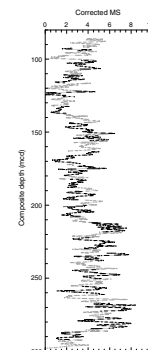
---

---

**T2.** Control points used for the construction of the TCMS age model, p. 17.

---

**F2.** The composite section for Pliocene Site 1085, generated by splicing corrected MS core data, p. 8.



tion is generated from core recovered from three holes and compensates for local variations in deposition by removing sections that are unlike the other two holes at that site. Because only two holes were drilled at Site 1085, there is potential for some error in the composite record. Berger et al. (1998) document an association between gas expansion and offset of MS data between holes in the Congo Fan region. Similarly, expansion is anticipated in the Cape Basin because of the presence of gases (notably methane). This expansion should add some noise, but smoothing should remove much of it. However, core growth, as measured by core offsets generated in the composite depth analysis, indicates that there is only an expansion of ~5% in this interval (Wefer, Berger, Richter, et al., 1998). Even if the core is disturbed by gas expansion, the time represented is probably minimal. Assuming an 8-cm/k.y. average sedimentation rate, even a very long interval of expanded sediments (e.g., 40 cm) would only represent 5 k.y., significantly less than the sampling required to identify 41- and 100-k.y. cyclicity.

**BIOSTRATIGRAPHIC MODEL**

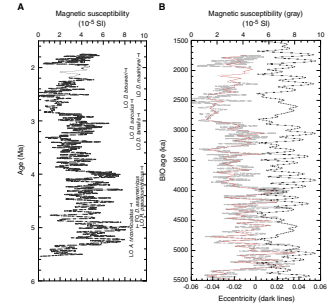
Shipboard calcareous nannofossil datums (Table T1) were used to develop the preliminary biostratigraphically based age model (Fig. F3A). The BIO age model (Fig. F3A) was developed by applying a linear sedimentation rate between calcareous nannofossil datums to the composite Site 1085 MS core data (Fig. F2). Planktonic foraminifer biostratigraphic datums were not used to constrain the ages for this interval mainly because the biostratigraphic resolution of the calcareous nannofossil group is superior in this interval to that of the planktonic foraminifers (see Wefer, Berger, Richter, et al., 1998, for further discussion). One major drop in sedimentation rate is identified using the BIO model at ~103 meters composite depth (mcd) (~93 mbsf, between 2250 and 1950 ka) (Fig. F4). It is associated with a dark greenish gray unit in Hole 1085A (interval 175-1085A-11H-2, 48–100 cm) that maintains a sharp upper contact (91 mbsf) and a gradational lower contact with the light greenish gray unit that dominates this interval (Wefer, Berger, Richter, et al., 1998). The surface at ~103 mcd may be unconformable and, in this model, represents ~200 k.y. of missing time.

When the BIO model is compared to the eccentricity record (Fig. F3B), an ~100-k.y. peak is apparent, although spectral analysis documents that the power spectrum is shifted according to that of the eccentricity (Fig. F5A). The spectral variance of both the BIO age model (Table T3) and the eccentricity record for this interval (5.5–2 Ma) (Fig. F5A) are offset such that the 96- and 128-k.y. eccentricity peaks are centered at 77 and 88 k.y. in the BIO model, and the broad 407-k.y. peak in eccentricity is centered at 291 k.y. in the BIO model (Fig. F5A; Table T3). There is little spectral variance at periods <100 k.y. (Fig. F5A). The similarity in shape of the two curves suggests a strong relationship exists between MS and eccentricity, but tuning is required to confirm it.

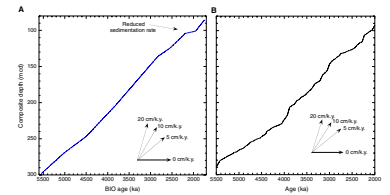
**ORBITALLY TUNED MODEL AND SPECTRAL ANALYSIS**

The BIO age model was improved by correlating the composite MS data with the eccentricity record of insolation to create an astronomically calibrated age model (the TCMS) (Fig. F6A, F6B, F6C; Table T2).

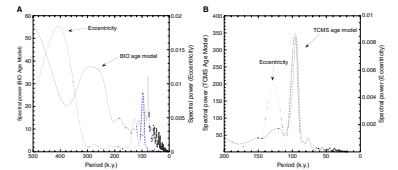
**F3.** The BIO age model, p. 9.



**F4.** Age-depths plot using the BIO and TCMS age models, with derived sedimentation rates, p. 10.

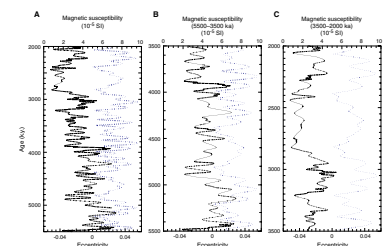


**F5.** Spectral analysis of eccentricity and the BIO and the TCMS age models, p. 12.



**T3.** Spectral analysis of three time series, p. 18.

**F6.** The TCMS age model with a nine-point moving window applied and compared to the eccentricity curve and BIO record, p. 13.



The TCMS shifts the correlation in two directions; the events deeper than ~265 mcd are correlated to peaks older than in the BIO model, and events above ~265 mcd are generally correlated to peaks younger than in the BIO model (Fig. F6D), although the unconformity at ~103 mcd suggested by the BIO model is slightly older (2300–2100 ka) in the TCMS model. Average sedimentation rates are 8 cm/k.y. with maximum rates in excess of 15 cm/k.y., occurring at 4400, 3900, 3000, and 2300 ka (Fig. F4B, F4C). There is an interval of dark gray sedimentation associated with the 3000-ka (~147 mcd; ~132 mbsf) and the 2300-ka (~115 mcd; ~104 mcd) events. Highest overall sedimentation rates occur between 4300 and 2800 ka

The TCMS model has a dominant peak at 94 k.y. and a secondary peak at 119 k.y., compared to the 96 and 128 k.y. anticipated for the eccentricity curve (Fig. F5B). There is also a significant peak at 76 k.y. (Fig. F5B). Cross-spectral analysis reveals highest coherencies at 103- and 94.5-k.y. periodicities at a low phase lag (Table T4), with additional significant elevated coherencies at 130 and 77 k.y. (Fig. F5B; Table T4). There is only moderate coherency at the 41- and 19-k.y. cycles and very low coherency at 23-k.y. periodicity (Fig. F5B; Table T4).

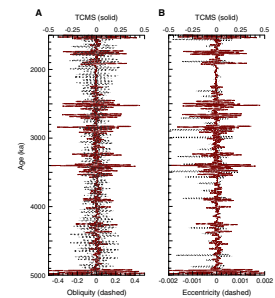
## ORBITAL CONTROL ON DEPOSITION

The spectral analysis suggests that eccentricity controls sedimentation. To elucidate that relationship, a Gaussian filter was applied to the insolation records at eccentricity and obliquity periodicities and to the TCMS age model (Fig. F7). The filtered MS signal is dominant at times of reduced filtered obliquity (4000–3000 ka) (Fig. F7A) and at times of increased dominance of the filtered eccentricity signal (4000–3000 ka) (Fig. F7B). The onset of Northern Hemisphere glaciation (e.g., 3.1 to 2.5 Ma; Haug and Tiedemann, 1998) is clearly associated with obliquity. The obliquity signal is strong between 3000 and 2500 ka; whereas, the eccentricity signal is reduced. Yet the 41-k.y. periodicity is not a dominant signal in the MS record in the Cape Basin despite the fact that Site 1085 is influenced by both Northern and Southern Hemisphere high-latitude climate changes (e.g., North Atlantic Deep Water impacts Antarctic Intermediate Water, but Antarctic glaciation impacts the position of the polar front, where Antarctic Intermediate Water is formed). One major problem may be the dual climate influences at this site. For example, glacial-interglacial periods are linked to changes in high-latitude Northern Hemisphere changes in obliquity. However, the Southern Hemisphere does not always experience synchronous changes in mean insolation and is sometimes out of phase with the Northern Hemisphere. Thus, different phases of the obliquity cycle forcing an oceanographic response in the Southern Hemisphere might thereby obscure the Northern Hemisphere connection.

Another problem may be that forcing at eccentricity periodicities may play a more important role in the onset of Northern Hemisphere glaciation than previously thought. The record of eccentricity changes from the more broad-shouldered events before and after (>5500 to 4300 ka and 3000 to 2000 ka), to events with higher frequency and greater amplitude (4300 to 3000 ka) (Fig. F6A, F6B, F6C). There is also a correlation between the change in character of the eccentricity curve and increased sedimentation rates (Fig. F4) that suggests a depositional response to orbital variation at the eccentricity periodicity. Close examination of the filtered record of insolation at eccentricity periodic-

**T4.** Cross-spectral analysis of the TCMS age model and the eccentricity record of insolation, p. 19.

**F7.** Gaussian filter applied to the TCMS and the obliquity and eccentricity records, p. 15.



ities reveals a higher frequency oscillation at greater magnitude between ~4000 and 2800 ka (Fig. F7B), coincident with a decreased dominance of the obliquity signal (Fig. F7A) and an increase in the dominance of the TCMS record (Fig. F7A, F7B). This time period is associated with fluctuations in Northern Hemisphere ice-sheet growth. Haug and Tiedemann (1998) have suggested that the onset of Northern Hemisphere glaciation began as early as 4.1 Ma but proceeded as a series of false starts, with ice-sheet growth waning in response to reduced-amplitude obliquity fluctuations. They find potential growth events occurring between 4.1 and 3.9 Ma and 3.5 and 3.3 Ma, periods of high dominance of the insolation at the eccentricity periodicity (Fig. F7B) and of increased dominance in the MS record (Fig. F7A, F7B).

## **CONCLUSIONS**

Eccentricity modulates the MS signal in the Cape Basin. The highest dominance of the filtered MS record is coincident with the highest dominance of the filtered eccentricity record (Fig. F7B) but not of the highest dominance of the filtered obliquity record (Fig. F7A). Although variations in obliquity are thought to control the onset of Northern Hemisphere glaciation, it is equally likely that variations in insolation at the eccentricity periodicity played an important role. Northern Hemisphere variation at the obliquity periodicity may influence the region but may be obscured by antiphase Southern Hemisphere paleoceanographic responses. Thus, it is not possible to separate the signal using only MS data, and a multiproxy approach is necessary to separate Northern and Southern Hemisphere components of the signal.

## **ACKNOWLEDGMENTS**

This research used samples and/or data provided by the Ocean Drilling Program (ODP). ODP is sponsored by the U.S. National Science Foundation (NSF) and participating countries under management of Joint Oceanographic Institutions (JOI), Inc. Funding for this research was provided by JOI/USSSP grant number F000825 (Christensen) and NERC grant number GST/02/2690 (Maslin).

## **REFERENCES**

- Berger, W.H., Wefer, G., Richter, C., and Shipboard Scientific Party, 1998. Color cycles in Quaternary sediments from the Congo Fan region (Site 1075): a statistical analysis. *In* Wefer, G., Berger, W.H., and Richter, C., et al., *Proc. ODP, Init. Repts.*, 175: College Station, TX (Ocean Drilling Program), 561–567.
- Christensen, B., Maslin, M., Kalbas, J., and Ellershaw, M., 1999. The surface and deep water response in the Cape Basin to the progressive closure of the Isthmus of Panama and the associated enhanced thermohaline circulation. *Eos, Trans., Am. Geophys. Union*, 80:589.
- Haug, G.H., and Tiedemann, R., 1998. Effect of the formation of the Isthmus of Panama on Atlantic Ocean thermohaline circulation. *Nature*, 393:673–676.
- Kalbas, J., Christensen, B.A., Meyers, P., Maslin, M., and Murray, R., 1999. The impact of the onset of Northern Hemisphere glaciation on South Atlantic Site 1085, Cape Basin, ODP Leg 175, *Eos, Trans., Am. Geophys. Union*, 80:567.
- Laskar, J., 1990. The chaotic motion of the solar system: a numerical estimate of the size of the chaotic zones. *Icarus*, 88:266–291.
- Paillard, D., Labeyrie, L., and Yiou, P., 1996. Macintosh program performs time-series analysis. *Eos*, 77:379.
- Wefer, G., Berger, W.H., and Richter, C., et al., 1998. *Proc. ODP, Init. Repts.*, 175: College Station, TX (Ocean Drilling Program).

**Figure F1.** Ocean Drilling Program Sites 1075–1087 drilled during Leg 175. Site 1085 is located in the northern part of the Cape Basin at a water depth of 1713 m. The study area is fed by three surface water currents (Benguela Current, Antarctic Circumpolar Current, and Agulhas Current) and bathed by Antarctic Intermediate Water (AAIW) at depth. Deep Sea Drilling Project (DSDP) sites are also shown.

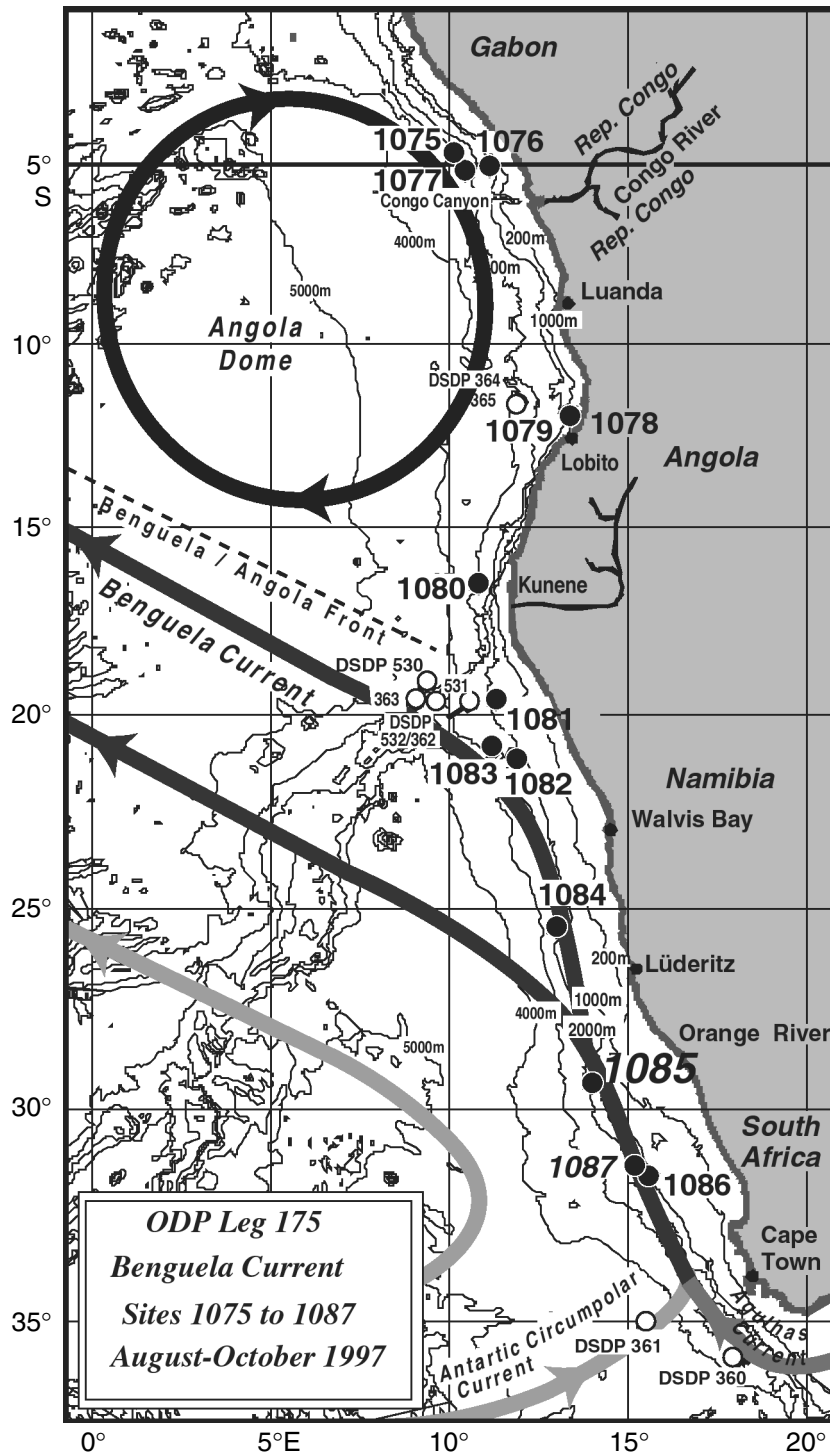


**Figure F2.** The composite section for Pliocene Site 1085, generated by splicing corrected magnetic susceptibility (MS) core data from Holes 1085A and 1085B. Contributions from Hole 1085A are shown in black; Hole 1085B, in gray. A nine-point smoothing function was applied to the corrected MS data.

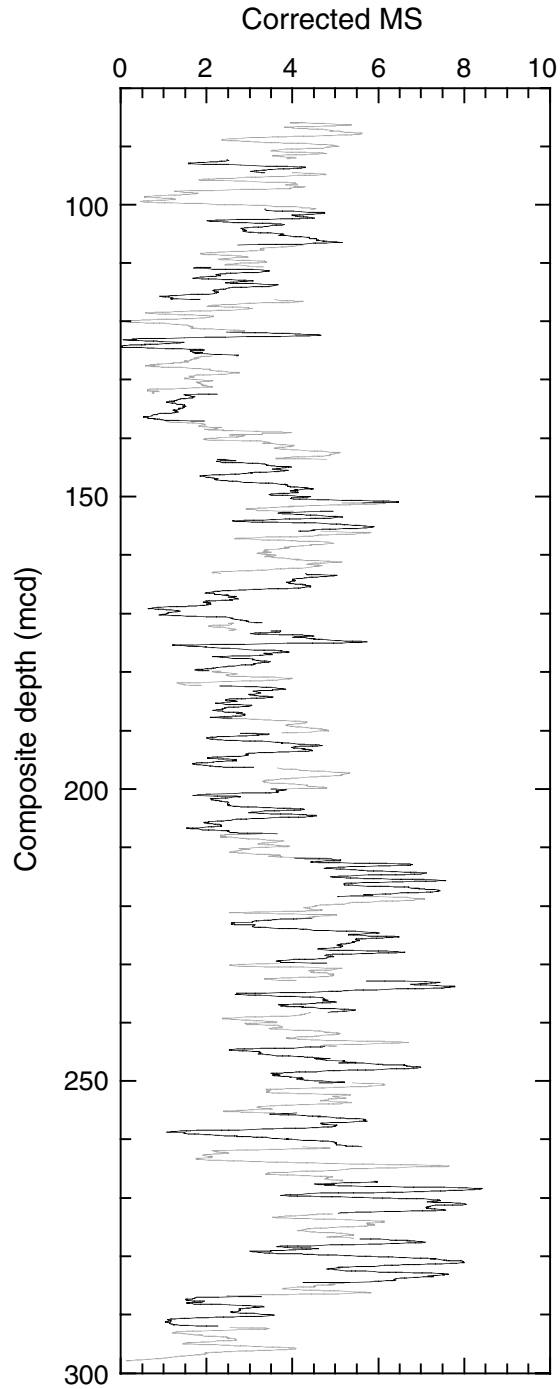


**Figure F3.** **A.** The biostratigraphic (BIO) age model. A nine-point moving window was applied once to the composite magnetic susceptibility data. Calcareous nannofossil datums used to determine the age model are shown. LO = last occurrence, FO = first occurrence. **B.** Comparison of BIO age model and the eccentricity record. A cubic spline smoothing function (heavy black line) was applied to the MS data (plotted in gray). Approximately 100- and 400-k.y. cycles exist in the record but do not correlate well with the eccentricity curve without tuning.

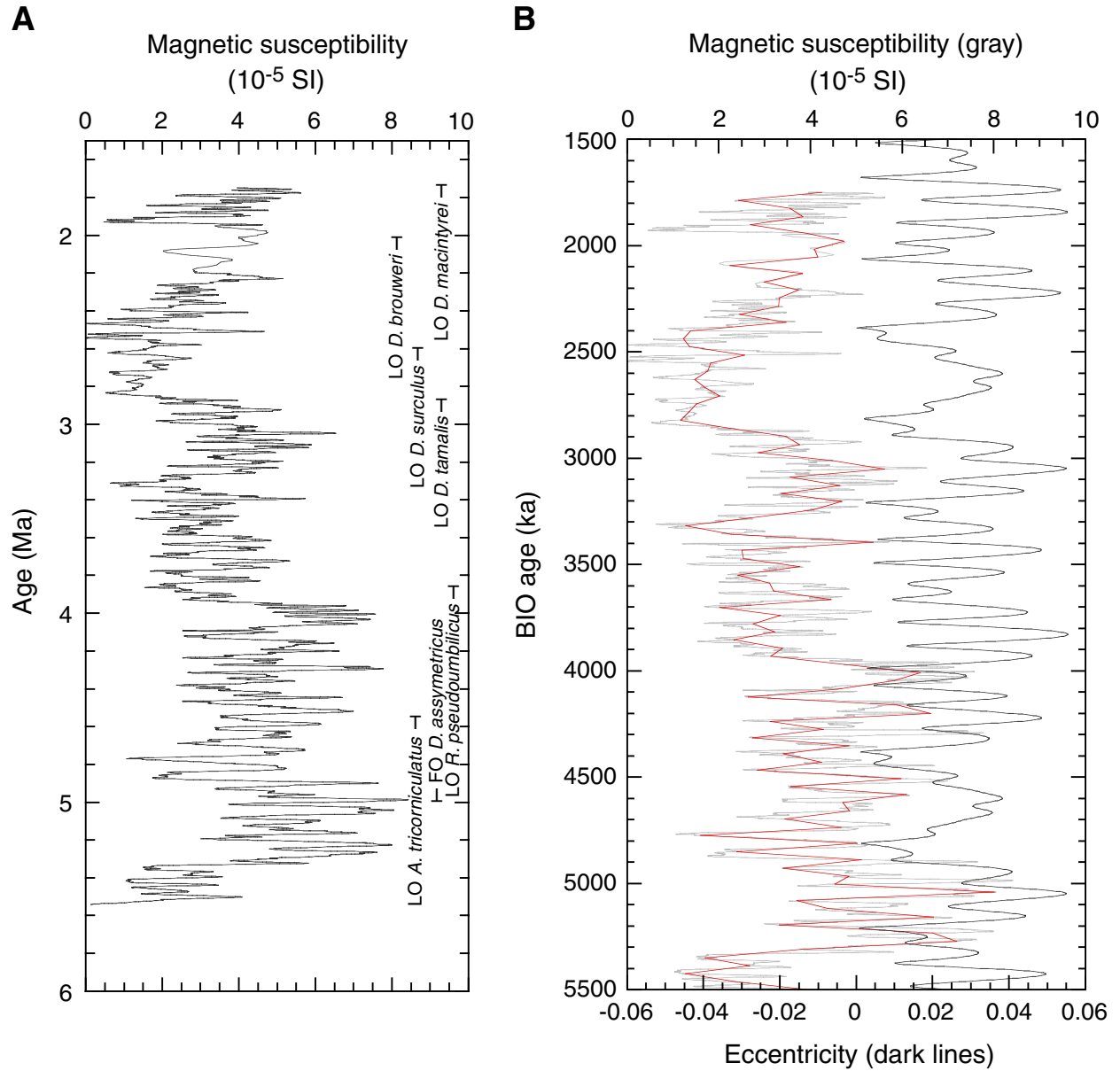


**Figure F4.** A. Age-depth plot using the biostratigraphic (BIO) age model only. Note the reduced sedimentation rate at ~100 m (~2.5 Ma). B. Age-depth plot using the tuned core magnetic susceptibility (TCMS) age model only. Note the increased variability in sedimentation rate. (Continued on next page.)

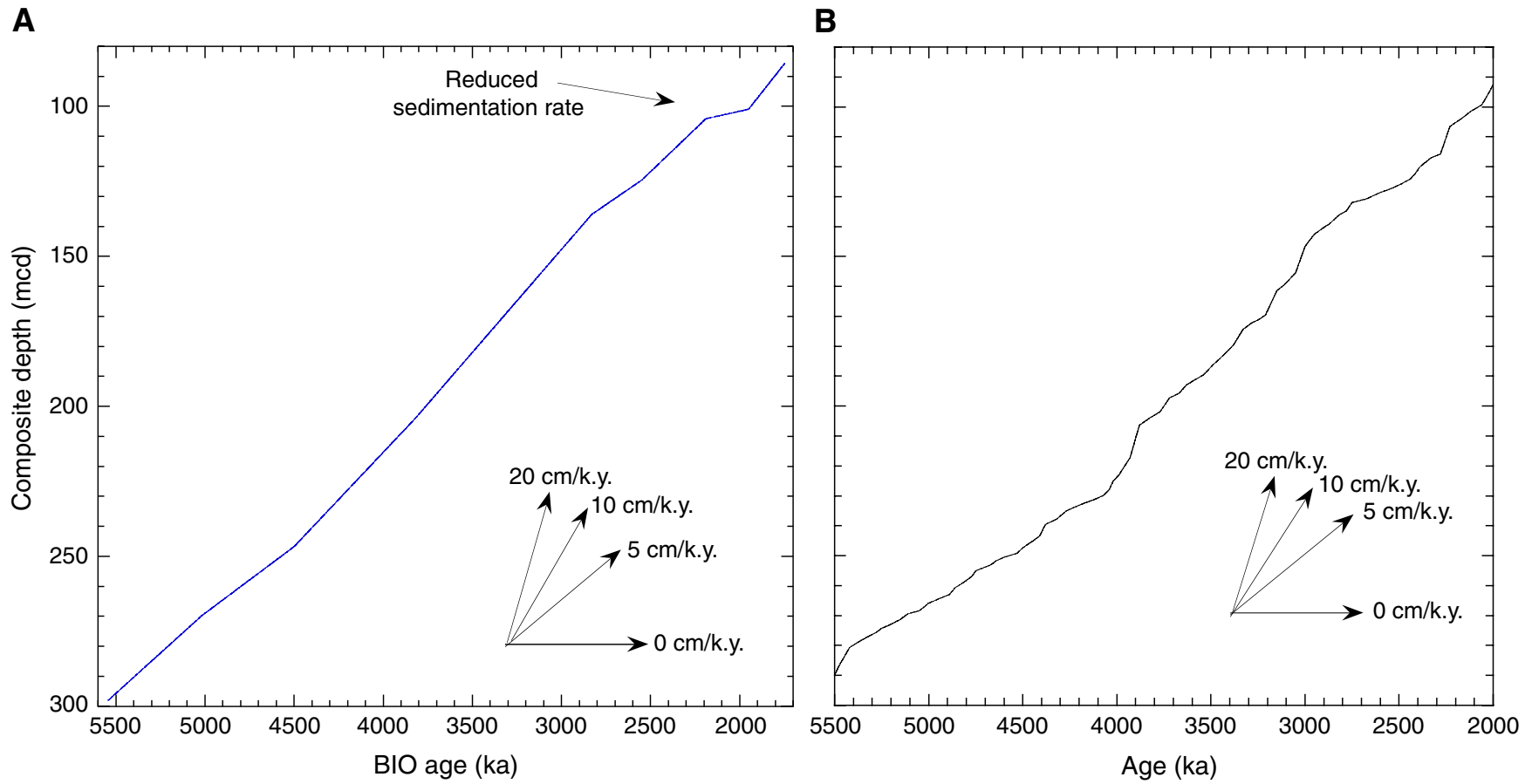
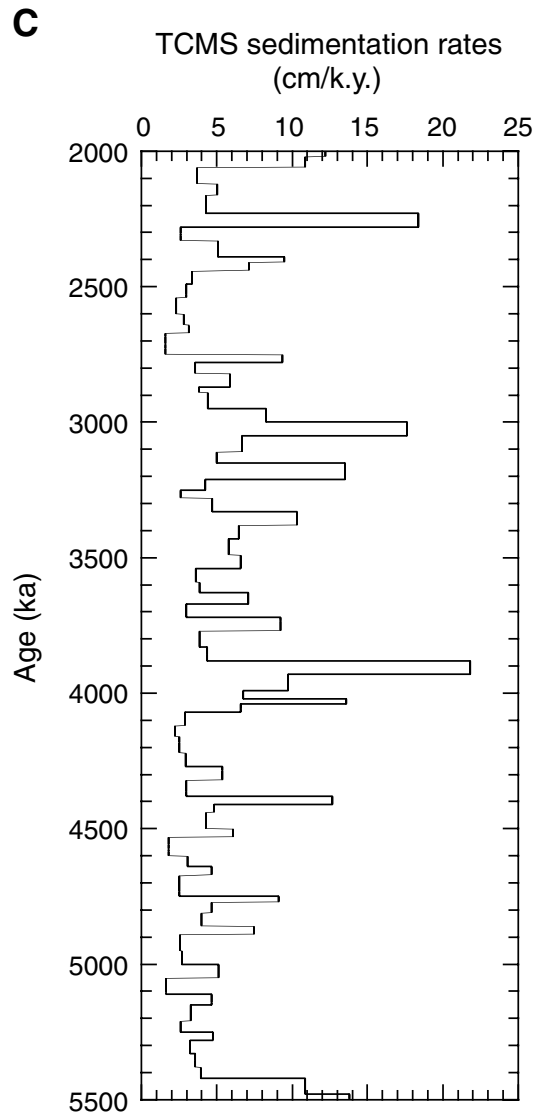
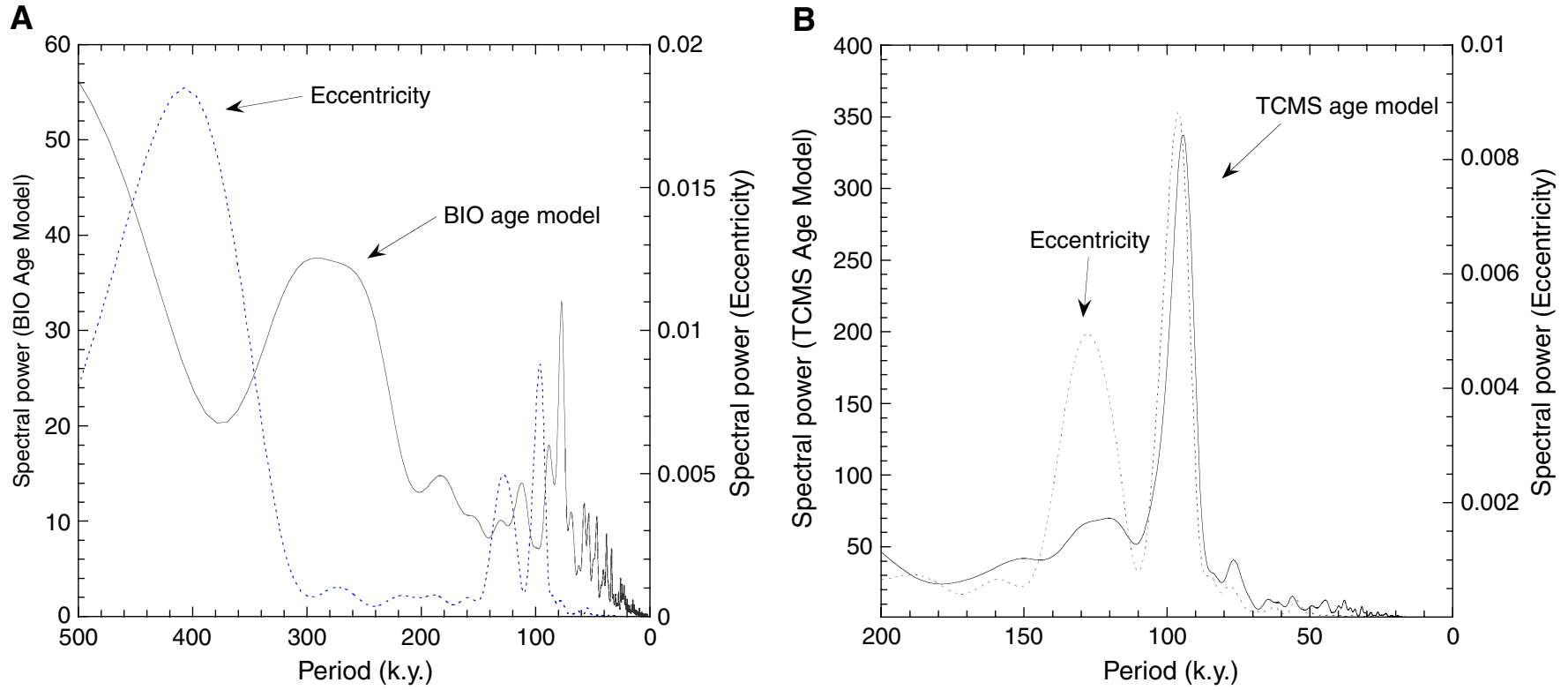


Figure F4 (continued). C. Sedimentation rates derived from the TCMS age model.



**Figure F5.** Spectral analysis of (A) eccentricity and the biostratigraphic (BIO) age model and of (B) eccentricity and the tuned core magnetic susceptibility (TCMS) age model. The following apply to the BIO age model: bandwidth = 0.00131, number of lags = 2278, step = 2 k.y. The following apply to the TCMS age model: linear trend was removed, bandwidth = 0.00139, number of lags = 2149, step = 2 k.y.



**Figure F6.** A. The tuned core magnetic susceptibility (TCMS) age model with a nine-point moving window applied and compared to the eccentricity curve (dashed lines) in this same interval. B, C. The TCMS record (dashed) is magnified over two intervals ([A] 5500–3500 ka and [B] 3500–2000 ka) to show detail and to compare to the eccentricity curve (solid). (Continued on next page.)

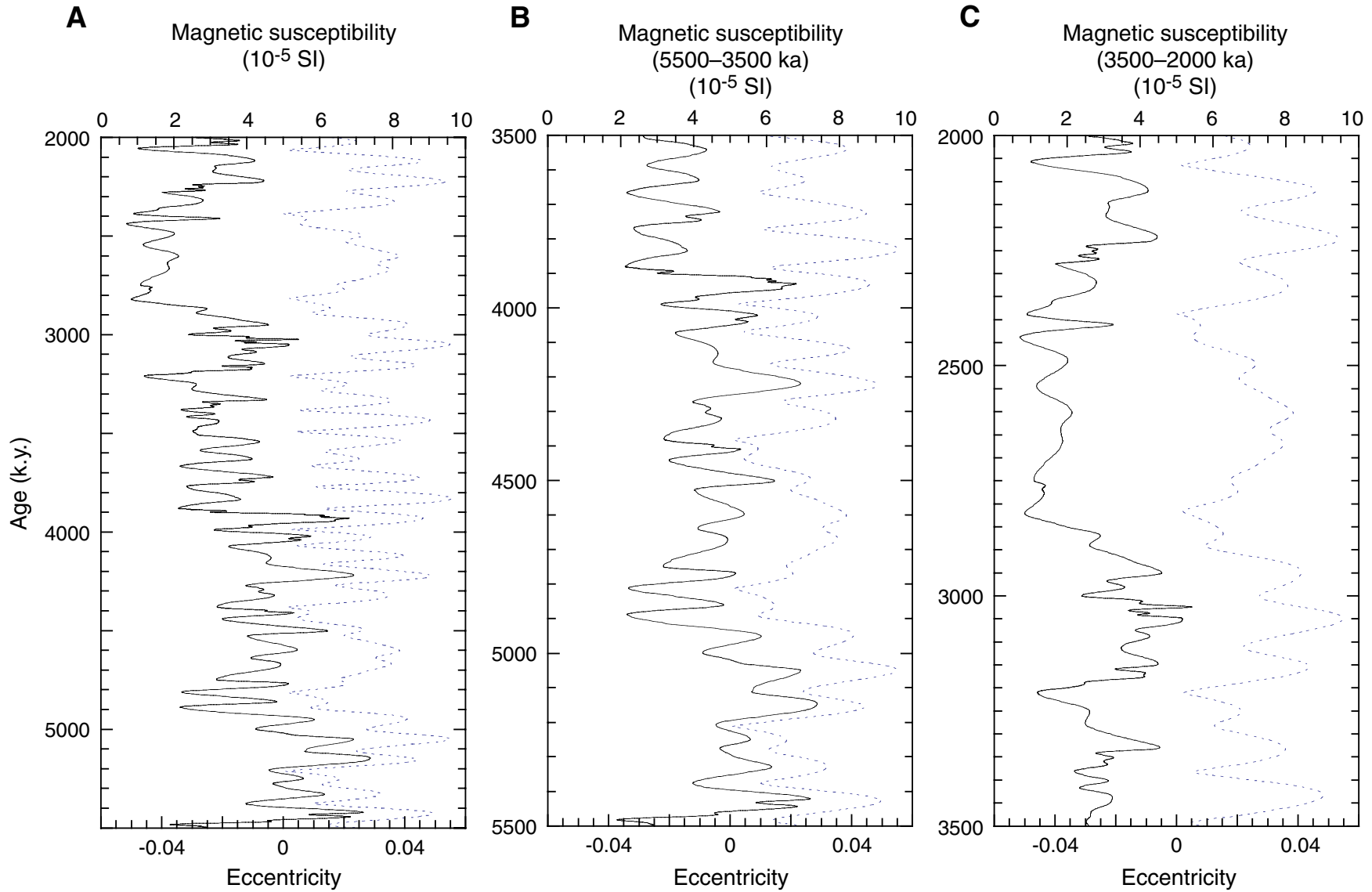


**Figure F6 (continued). D.** The TCMS model (solid) is compared to the BIO age model record (dashed). The major difference between the models occurs between 5000 and 4000 ka, whereby the BIO model (solid) is younger than the TCMS model (dashed). The data were tuned nine times with a nine-point filter to remove the subcentricity variability and enhance the correlation to the eccentricity curve.

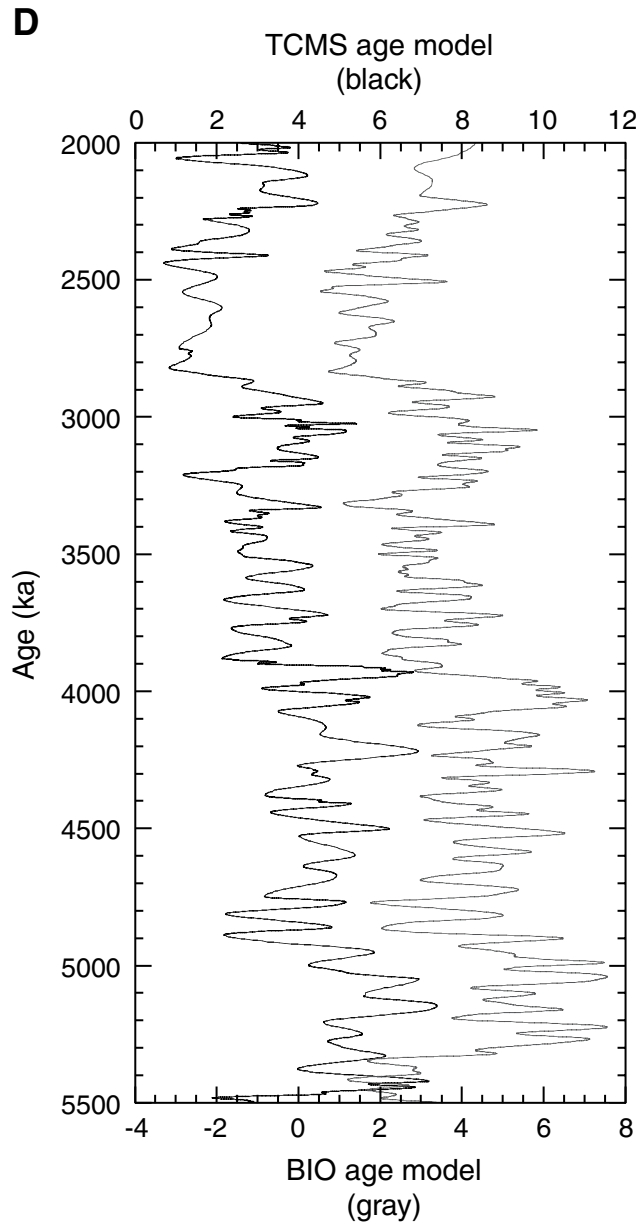


**Figure F7. A.** Gaussian filter applied to the tuned core magnetic susceptibility (TCMS) age model and the (A) obliquity and (B) eccentricity records of insolation. The following apply to the filtered data: bandwidth = 0.02,  $f = 0.05$ . The data were centered at 20 between periods 14.285714 and 33.3333.

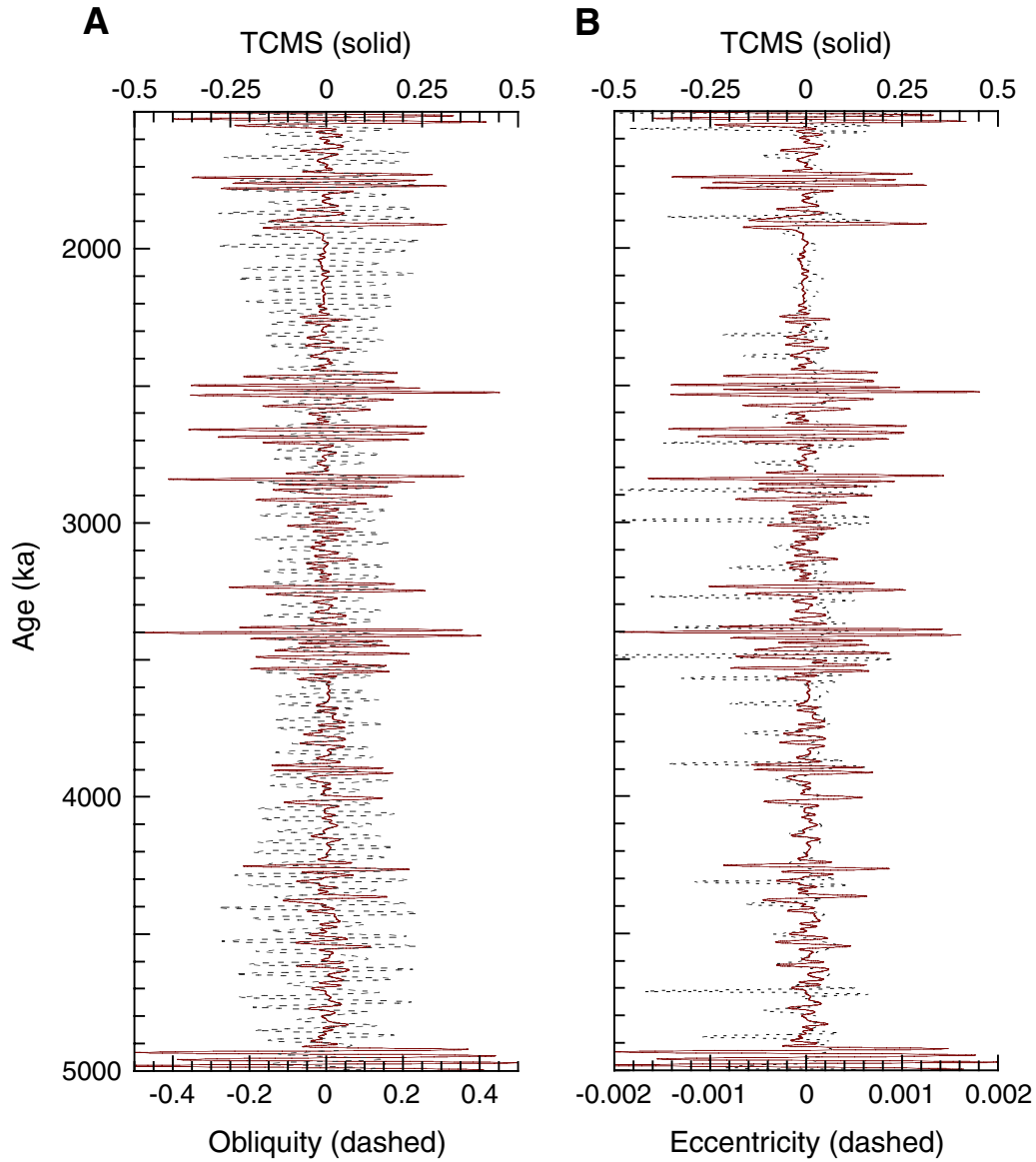


**Table T1.** Shipboard biostratigraphic datums.

Datum event	Age (Ma)	Core, section, interval (cm)		Depth (mbsf)		
		Top	Bottom	Top	Bottom	Mean
LO <i>Calcidiscus macintyre</i>	1.67	8H-CC	9H-2, 140	68.37	73.10	70.74
LO <i>Discoaster brouweri</i>	1.95	10H-CC	11H-3, 10	89.67	92.30	90.99
LO <i>Discoaster surculus</i>	2.55	12H-CC	13H-CC	108.49	117.82	113.16
LO <i>Discoaster tamalis</i>	2.83	13H-CC	14H-CC	117.82	127.45	122.64
LO <i>Reticulofenestra pseudoumbilicus</i>	3.82	20H-CC	21H-CC	183.96	193.63	188.80
LO <i>Amaurolithus tricorniculatus</i>	4.50	24H-CC	25H-CC	221.90	230.99	226.45
FO <i>Discoaster asymmetricus</i>	5.02	26H-CC	27H-CC	241.53	250.87	246.20
LO <i>Discoaster quinquerramus</i>	5.54	32H-CC	33H-CC	296.87	304.90	300.89

Notes: Calcareous nannofossil datums were used to develop the biostratigraphic age model and to provide an estimate of stratigraphic position for the tuned core magnetic susceptibility model. LO = last occurrence, FO = first occurrence.

**Table T2.** Control points used for the construction of the TCMS age model.

Depth (mcd)	Age (k.y.)	Depth (mcd)	Age (k.y.)
92.54	2000	206.39	3880
94.98	2020	217.29	3930
99.32	2060	223.13	3990
101.54	2120	225.15	4020
103.56	2160	227.87	4040
106.56	2230	229.85	4070
115.74	2280	231.29	4120
117.04	2330	232.17	4160
120.08	2390	233.67	4220
121.98	2410	235.13	4270
124.12	2440	237.82	4320
125.80	2490	239.60	4380
127.28	2540	243.40	4410
128.66	2600	244.84	4440
129.78	2640	247.40	4500
130.72	2670	249.22	4530
131.98	2750	250.56	4600
134.78	2780	251.70	4640
136.20	2820	253.10	4670
139.14	2870	255.10	4750
139.90	2890	256.92	4770
142.54	2950	258.78	4810
146.66	3000	260.78	4860
155.48	3050	263.02	4890
159.48	3110	264.56	4950
161.48	3150	265.90	5000
169.59	3210	268.46	5050
171.29	3250	269.44	5110
172.07	3280	271.30	5150
174.43	3330	273.26	5210
179.59	3380	274.30	5250
182.83	3430	275.72	5280
186.31	3490	277.34	5330
189.61	3540	279.12	5380
191.41	3590	280.70	5420
192.95	3630	287.22	5480
195.79	3670	289.98	5500
197.27	3720		
201.89	3770		
204.21	3830		

Note: TCMS = tuned core magnetic susceptibility.

**Table T3.** Spectral analysis of three time series.

Time series analyzed	Period (k.y.)	Frequency (cycles/k.y.)	Spectral power
BIO	88.6	0.01128668	18.03
	77.3	0.01293661	33.04
	53.7	0.01862197	10.80
	57.6	0.01736111	11.88
	46.6	0.02145923	10.48
	291.4	0.00343171	37.63
TCMS	94.1	0.01062699	337.33
	119.8	0.00834725	69.84
	76.7	0.01303781	40.80
	64.4	0.01552795	13.28
	56.2	0.01779359	15.42
	44.6	0.02242152	12.80
	39.9	0.02506266	8.70
	31.9	0.03134796	8.30
Eccentricity	96.3	0.01038422	0.00882
	128.0	0.00781250	0.00495
	407.0	0.00245700	0.01849

Notes: The following apply to the biostratigraphic age model (BIO): bandwidth = 0.00131, number of lags = 2278, step = 2 k.y. The following apply to the tuned core magnetic susceptibility (TCMS) age model: linear trend was removed, bandwidth = 0.00139, number of lags = 2149, step = 2 k.y.

**Table T4.** Cross-spectral analysis of the TCMS age model and the eccentricity record of insolation.

Period (k.y.)	TCMS vs. eccentricity	Coherence	Phase lag
128	65.613	0.86844	-0.12493
119	69.527	0.85330	0.10572
102	112.90	0.90994	-0.15452
96	313.65	0.90769	0.04724
94	329.98	0.91044	0.20036
76	40.649	0.83381	-0.24443
41	5.1343	0.43663	-0.16647
23	3.5364	0.099928	-2.45170
19	2.1719	0.32747	0.20036

Note: The tuned core magnetic susceptibility (TCMS) vs. eccentricity analysis was performed at 95% confidence level using a step of 0.5 k.y., 2100 lags, and a bandwidth of 0.00142 on linear detrended data.